

3D Face Recognition using Mapped Depth Images

Gang Pan, Shi Han, Zhaohui Wu and Yueming Wang

Department of Computer Science
Zhejiang University, Hangzhou, 310027, P.R.China
{gpan, hanshi, wzh, ymingwang}@zju.edu.cn

Abstract

This paper addresses 3D face recognition from facial shape. Firstly, we present an effective method to automatically extract ROI of facial surface, which mainly depends on automatic detection of facial bilateral symmetry plane and localization of nose tip. Then we build a reference plane through the nose tip for calculating the relative depth values. Considering the non-rigid property of facial surface, the ROI is triangulated and parameterized into an isomorphic 2D planar circle, attempting to preserve the intrinsic geometric properties. At the same time the relative depth values are also mapped. Finally we perform eigenface on the mapped relative depth image. The entire scheme is insensitive to pose variance. The experiment using FRGC database v1.0 obtains the rank-1 identification score of 95%, which outperforms the result of the PCA base-line method by 4%, which demonstrates the effectiveness of our algorithm.

1 Introduction

The automatic face recognition based on 2D image has been actively researched during the past three decades, and various techniques have been presented [1, 2]. However, traditional face recognition methods appear to be sensitive to variations in pose, illumination and expression. These methods' limitations are derived from the limited facial information in the planar image. In nature, 2D image is the projection of the 3D human face onto a certain plane. This intrinsic weakness of planar image makes it hard to cope with the problems.

This paper focuses on face recognition using 3D facial surface. The face data have the following advantages compared with 2D face data: firstly, the illuminating has less effect on the depth information. Secondly, the variation of facial pose doesn't lose any face information. Thirdly, the 3D data have more clues to handle expression change than 2D image since they preserve the 3D geometry information. Recently, it becomes evident that the use of 3D facial data

could be of great help [3, 29].

The current techniques in 3D acquiring system make it practical to quickly and accurately build the face model. But the activities to exploit the additional information in 3D data to improve the accuracy and robustness of face recognition system are still expected to be addressed.

1.1 Previous Work

The previous work utilizing 3D information for face recognition could be categorized into four groups:

Feature based: Curvature is the intrinsic local property of curved surface. The local shape could be determined by its primary curvature and direction [5]. Therefore, most of the early studies used curvature to analyze the features of 3D facial data [7, 8, 9, 10]. Gordon [8, 9] presented a template-based recognition system involving descriptors based on curvature calculations from range image data. The sensed surface regions were classified as convex, concave and saddle by calculating the minimum and maximum normal curvatures. Then locations of nose, eyes, mouth and other features were determined, which were used for depth template comparison. An approach to label the components of human faces was proposed by Yacoob [10]. Qualitative reasoning about possible interpretations of the components was performed, followed by consistency of hypothesized interpretations.

Spatial matching based: Recognizing was performed via matching facial surface or profile directly in 3D Euclidean space [14, 22, 23, 24, 26]. This kind of approaches generally assume that the facial surface is a rigid object so that are not competent for the recognition among the models with expressions.

Shape descriptor based: It exploits the shape representation or shape descriptor to achieve the recognition task in the representation domain. For instance, Chua [13] used point signature - a representation for free-form surfaces for 3D face recognition, in which the rigid parts of the face

of one person are extracted to deal with different facial expressions. Wang [25] used a new shape representation called Local Shape Map for 3D face recognition. This kind of technique is simple and somewhat robust to small perturbations. However, its classification rate is considered to be low.

Recover-and-synthesis based: For this kind of methods, their probes still are 2D images but not 3D data. The partial 3D information was recovered from the 2D image, then the facial image in virtual view was synthesized for recognition [12, 16, 28] or the recognition task was accomplished with the recovered parameters [11]. This type of approaches do not make full use of those online-available 3D information.

1.2 Motivation

Human face is a non-rigid object attributed to deformations from the facial expressions. Although the 3D facial data have more clues for recognition than 2D image, the processing of 3D data generally requires more expensive computational cost. On the other hand, there are many analysis methods for 2D image, while it is great difficulty to handle 3D face models directly for its irregularity in space. So a suitable way is to convert the useful 3D information into a 2D domain with important discriminative characteristics preserved.

Thus, in this paper, we attempt to find a mapping Ψ between a given facial surface S and an isomorphic planar triangulation $U \in R^2$ that best preserves the original, discriminative characteristics of S .

If a one-to-one mapping from 3D facial surface to an isomorphic planar space is provided, the recognition task could be allowed to perform directly on the flat domain rather than on the curved surface. Bronstein[27] et al. proposed the bending-invariant canonical representation for 3D surfaces. However, such a mapping is not a direct way from 3D space to 2D domain. The mapping scheme used in our algorithm, from 3D spatial space to an isomorphic planar space provides a tradeoff among different features of the surface while trying to preserve them, which is more flexible and adaptive.

This paper presents a novel 3D face recognition approach based on planar parametrization. Firstly, the region of interest which contains the most significant features of a human face is automatically selected. Then we find the base plane through the nose tip for calculating the relative depth, which is pose-invariant. After that the ROI in range data is triangulated and mapped into an isomorphic 2D planar circle, preserving the intrinsic geometric properties,

with the relative depth being mapped as well. Finally we apply the eigenface method on the mapped depth images to achieve the recognition task.

The rest of the paper is organized as follows. The next section introduces our automatic ROI selecting algorithm. Section 3 describes the distortion criterion for mapping and how to map the 3D facial surface and features into an isomorphic planar triangulation. Section 4 presents the experimental results. Conclusions are drawn in the last section.

2 Extraction of ROI

Given a large database such as FRGC dataset, the first thing is to accurately and efficiently pick out the region of interest(ROI) on each human face. Although FRGC dataset provides such landmarks as nose tip, left eye and right eye for each 3D facial model, we do not use the additional information. Instead, an automatic extraction of ROI is introduced.

Our method to automatically extract ROI is based on the following ideas:

1. The ROI is in a sphere centered at the nose tip.
2. The nose tip is a point on the curve of central profile, with the maximum distance to the line through both curve ends.
3. The central profile is in the symmetry plane of the face surface, namely the curve of the central profile is the intersection of the symmetry plane and the facial surface.

And we try to solve the problem in the reverse sequence of the deduction above. The algorithm consists of two main steps: symmetry plane detection and the nose tip localization.

2.1 Finding Symmetry Plane of Facial Surface

In our previous work[23], we have proposed an effective method to find symmetry plane of facial surface. Here we apply and improve it to detect the curve of the central profile from human face model.

Given a point set S of a human face range data, we can get its mirror S' subject to an initial approximate symmetry plane M . After S' has been registered to S , S' is translated and rotated into S'' . Therefore S and S'' compose a new point set \bar{S} ,

$$\bar{S} = S + S'' \quad (1)$$

where \bar{S} is self-symmetric, and the symmetry plane A runs through the bisector of each corresponding pair of points in

S and S'' . Let \mathbf{P} is any point in S and \mathbf{P}'' is its mirrored point in S'' , then symmetry plane A will be

$$A = \{\mathbf{x} | \langle \mathbf{x} - (\mathbf{P} + \mathbf{P}'')/2, \mathbf{P} - \mathbf{P}'' \rangle = 0\} \quad (2)$$

where $\langle \cdot, \cdot \rangle$ means inner product. Details refer to [23].

As [23], we introduce the iterative closest points(ICP) method to do the registration. But considering the convergence problem of ICP, the initial mirror plane M mentioned above should be properly selected. Observing the character of human faces, we find that the general shape of the face is like part of the ellipsoid surface, with the longest axis in top-bottom direction and the shortest axis pointing to the nose tip. Hence we do the principle component analysis on three dimensional point set S , and get the average point $\bar{\mathbf{p}}$ and three eigenvectors \mathbf{v}_1 , \mathbf{v}_2 and \mathbf{v}_3 , which are in the descending order according to their eigenvalues. Thus \mathbf{v}_1 is approximately the up-side direction of the face and \mathbf{v}_3 points outside the face. So we can define the initial symmetry plane M as

$$M = \{\mathbf{x} | \langle \mathbf{x} - \bar{\mathbf{p}}, \mathbf{v}_2 \rangle = 0\} \quad (3)$$

to help the convergence of ICP. Finally we calculate the intersection of resulted symmetry plane A and the triangulated surface of S to get the central profile curve C . Figure 1 shows the procedure of symmetry plane detection.

2.2 Detecting Nose Tip

After we have calculated the central profile curve C , we locate the position of the nose tip as follows. Let P_1 and P_2 be the start and end of C , and L is the line segment between P_1 and P_2 , we define the nose tip N as

$$N = \arg \max_{P \in C} \{dist(P, L)\} \quad (4)$$

where $dist(\cdot, \cdot)$ is the Euclidean distance function from a point to a line segment.

Then we could make a sphere centered with a certain radius at the detected nose tip N , and define the ROI as the set of points in both S and the sphere. The nose tip localization and ROI cropping is shown in Fig. 2

Finally, we triangulate the ROI with the Delaunay method and simplify it using mesh optimization[30] to reduce the calculation complexity.

3 Distortion Measurement and Flattening

For 2D image, there are general analysis methods for planar domain, for example, DFT and DCT are used widely in image processing. But it is great difficulty to handle 3D face models directly for its irregularity in space. So transforming

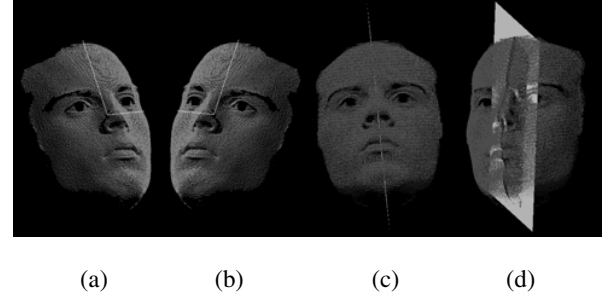


Figure 1: Symmetry plane detection. (a) is the original model and the three eigen-directions after PCA, (b) the mirrored model, (c) and (d) is the detected symmetry plane.

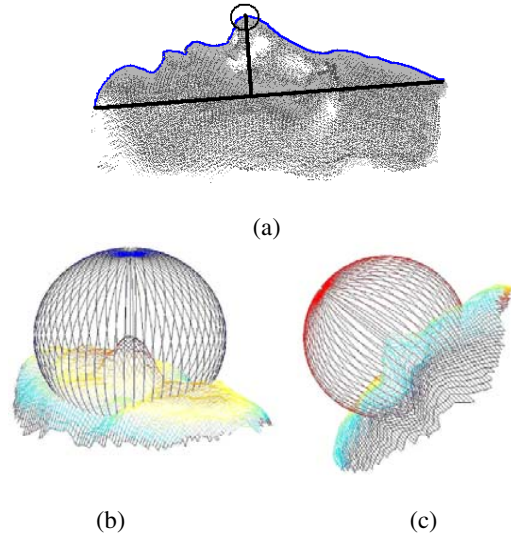


Figure 2: Facial ROI extraction. (a) the nose tip determined as the vertex on the central profile curve with the maximum distance to the line through both ends of the curve, (b) and (c) extraction of ROI using a sphere centered at the nose tip.

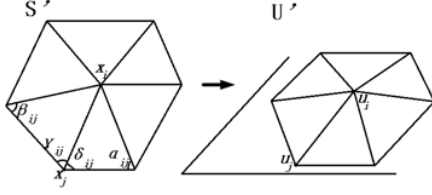


Figure 3: 3D 1-ring and its flattened version

the data to a regular domain is a feasible way. Given a facial surface S , a mapping Ψ between S and the isomorphic planar triangulation U is defined to preserve the original, discriminative characteristic of S .

The ideal mapping from a discrete curved surface to an isomorphic planar circle is expected to be isometric. The isometric transformation could be divided into two constraints: area-preserving and angle-preserving. In Desbrun [17], an algorithm which computes the discrete Dirichlet energy and applies conformal parametrization to interactive geometry remeshing, is adopted for harmonic energy minimization. A tradeoff is proposed when considering the angle-preserving and the area-preserving.

3.1 Distortion Measures

A function E is defined to measure distortion between S and U . So, it is obvious that the minimal distortion is obtained when $E(S, U)$ is minimum. In order to describe the measurement of distortion easily, let S' be a simple mesh consisting of a 1-ring neighborhood in 3D space, and let U' be an isomorph to S' in Fig. 3. Given fixed mapping boundary in Fig. 3, the 2D 1-ring distortion is only related to the center node u_i . If $\frac{\partial E}{\partial u_i} = 0$, the minimal distortion is achieved.

Two distortion metric E_A and E_X measure angle-preserving and area-preserving respectively, and they are mainly two properties for 3D mesh. The general distortion measurement can be defined as:

$$E = \alpha E_A + (1 - \alpha) E_X \quad 0 \leq \alpha \leq 1 \quad (5)$$

Gray[18] showed that the minimum of dirichlet energy E_A is attained for angle-preserving.

$$E_A = \sum_{\text{neighbouredges}(i,j)} \cot \alpha_{ij} |u_i - u_j|^2 \quad (6)$$

And in [17, 19], the authalic energy E_A is attained for area-preserving:

$$E_X = \sum_{j \in N(i)} \frac{(\cot \gamma_{ij} + \cot \delta_{ij})}{|x_i - x_j|^2} (u_i - u_j)^2 \quad (7)$$

Where $|u_i - u_j|$ is the length of the edge (i, j) in U' and $|u_i - u_j|$ in S' ; $\alpha_{ij}, \beta_{ij}, \gamma_{ij}$ and δ_{ij} are the angles shown in Fig. 3.

Since the energy is continuous and quadratic, while $\frac{\partial E}{\partial u_i} = 0$, we conclude the following equation based on Equ. 6 and Equ. 7:

$$\frac{\partial E_A}{\partial u_i} = \sum_{j \in N(i)} (\cot \alpha_{ij} + \cot \beta_{ij}) (u_i - u_j) = 0 \quad (8)$$

$$\frac{\partial E_X}{\partial u_i} = \sum_{j \in N(i)} \frac{(\cot \gamma_{ij} + \cot \delta_{ij})}{|x_i - x_j|^2} (u_i - u_j) = 0 \quad (9)$$

For the whole face model, the following equations can be deduced from all of the above:

$$M^A \begin{bmatrix} U_{\text{internal}} \\ U_{\text{boundary}} \end{bmatrix} = 0 \quad (10)$$

$$M_{ij}^A = \begin{cases} \cot(\alpha_{ij}) + \cot(\beta_{ij}) & \text{if } j \in N(i) \\ -\sum_{k \in N(i)} M_{ik}^A & \text{if } i = j \\ 0 & \text{otherwise} \end{cases} \quad (11)$$

and

$$M^X \begin{bmatrix} U_{\text{internal}} \\ U_{\text{boundary}} \end{bmatrix} = 0 \quad (12)$$

$$M_{ij}^X = \begin{cases} (\cot(\gamma_{ij}) + \cot(\delta_{ij})) / |x_i - x_j|^2 & \text{if } j \in N(i) \\ -\sum_{k \in N(i)} M_{ik}^X & \text{if } i = j \\ 0 & \text{otherwise} \end{cases} \quad (13)$$

For the general distortion measurement E in Equ. 5, the corresponding M combining M^A and M^X will be defined as:

$$M = \alpha M^A + (1 - \alpha) M^X \quad 0 \leq \alpha \leq 1 \quad (14)$$

3.2 Flattening of The Facial Surface

Given the mapped circle boundary U_{boundary} , the sparse linear system for parameterizations induces the following equation from section 2.1:

$$MU = \begin{bmatrix} M \\ 0 \quad I \end{bmatrix} \begin{bmatrix} U_{\text{internal}} \\ U_{\text{boundary}} \end{bmatrix} = \begin{bmatrix} 0 \\ C_{\text{boundary}} \end{bmatrix} = C \quad (15)$$

Parameterizing a triangular mesh onto the plane is just embedding a 3D position into the unit circle to each of the mesh vertices. Predefining the mapped boundary as a circle and setting the nose tip as center, there is only rotation's variable on the mapped plane. Since the boundary has been given, the sparse system is efficiently solved using generalized minimal residual algorithm [15].

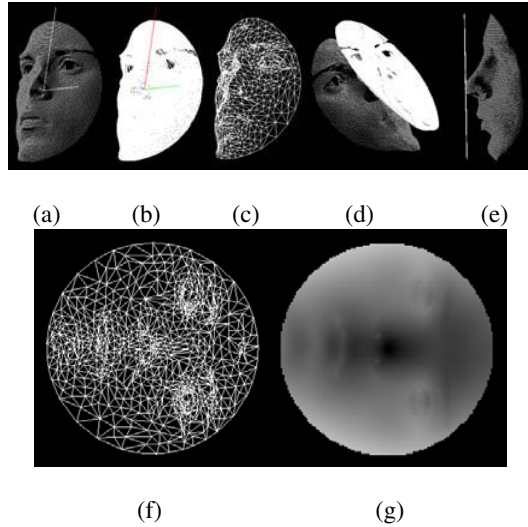


Figure 4: Illustration of the flattening mapping. (a) range data of ROI, (b) triangulated ROI, (c) simplified mesh of (b), (d) and (e) the reference plane by least square method, (f) the mapped ROI, (g) the mapped relative depth image.

3.3 Calculation of the Mapped Depth Image

Local geometry features of the surface could provide pose-independent information, but many features are too sensitive to noise. We adopt the relative depth value as the feature of each position on the face. To calculate the relative depth value, a reference plane is required. We apply the least square method to fit a plane to the point set of ROI, and translate it to the nose tip as the reference plane. Thus we get a pose-independent feature for each position on the face, by projecting onto the reference plane and get the relative depth image.

Through interpolation, we can calculate the feature of each point on the mapped disc. But there is still rotation difference for different faces. We remove the rotation in the following two steps.

1. Map the boundary vertex which is nearest to the start point of the central profile curve onto the right most point of the disc. And finish the flattening mapping.

2. Calculate the relative depth value and adjust the symmetry axis to horizontal direction.

After the above two steps, we indeed finish the regularization and registration of the mapped ROIs. The whole procedure of our algorithm is illustrated in Fig.4.

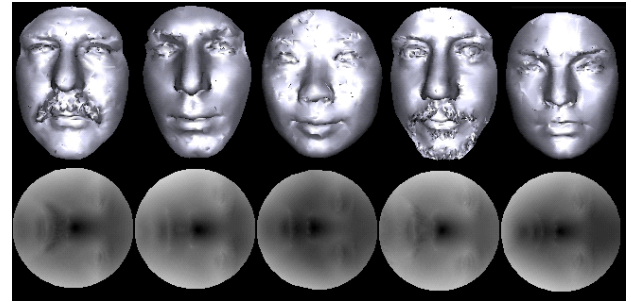


Figure 5: The first row shows the solid-rendering view of ROIs, and the second row shows their corresponding mapped relative depth image, which are feed to eigenface.

4 Experimental Results

Our experiments use the FRGC[29] database v1.0. There are 276 individuals and totally 943 face models, with 198 individuals who have more than 1 model. The facial regions are densely sampled, with the number of points ranging from about 20,000 to 110,000 for each. The leave-one-out rule is employed in the experiments.

We set the sphere radius mentioned in section 2 at 70 while cropping facial regions into ROIs, which include the most facial features. The cropped facial regions contain 12,500 to 59,000 points. We triangulate the points in ROIs with the Delaunay method, and simplify the mesh using mesh optimization[30] with an error tolerance of 10^{-6} , which reduce the number of points into about 1/20. The blending coefficient α in the flattening mapping for E_A and E_X is set to 0.5.

For the whole database of 943 face models, our facial ROI extraction approach successfully cropped the 934 nice ROIs which are proper for the subsequent steps. The 9 exceptions fall into two categories, the ones with too strange spike points, and the others with hair before or around the face region. We regularly sample the mapped ROIs into 128×128 matrices.

We carry out the experiments compared with the PCA baseline method to observe the performance of the proposed algorithm. And we also take the different rebuilding energy in the eigenface step, to determine the best parameter.

With the rebuilding energy of 0.99, our method achieves the identification rate of 95% with the EER of 2.83%.

The ROC curve is shown in Fig.6. Fig.7 and Fig.8 show the cumulative match characteristic and the rank 1 score respectively of the different rebuilding energy. The proposed algorithm obviously outperforms the traditional PCA method.

The time consumption for the models of minimum (20692 points) and maximum (126820 points), out of 943

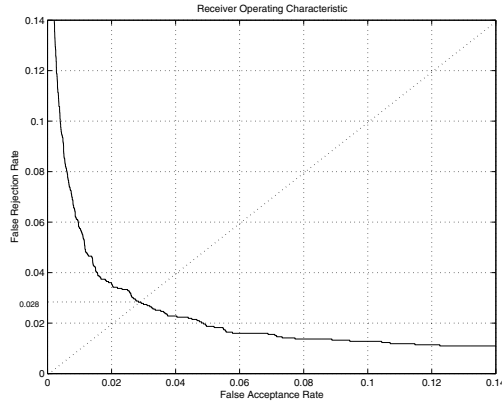


Figure 6: The ROC curve of the proposed method with ERR=2.83%.

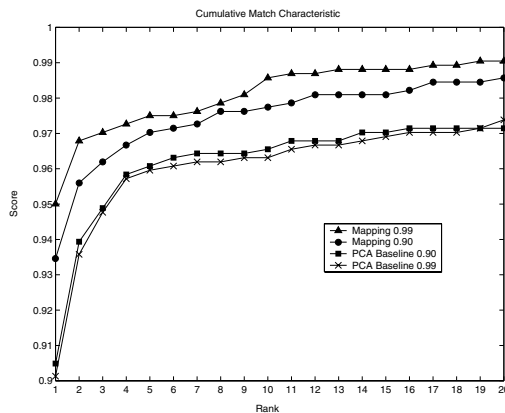


Figure 7: The CMC curves with different rebuilding energy for the proposed method and the PCA baseline.

models, is shown in Tab.4. Our system is running on PC of CPU P4 2.4GHz with 512MB DDR333 RAM.

5 Conclusion

We proposed a novel approach to face recognition for models in both mesh form and range data form. We firstly automatic extract the ROI of the face model, then flatten the ROI with the isomorphic mapping which preserves the intrinsic geometric properties of facial surfaces using planar parametrization, and get the relative depth image from the mapped ROI, finally we apply eigenface for the recognition. The proposed algorithm is insensitive to variation of the facial model's pose. Experimental results demonstrate that the our algorithm performs well on the FRGC database v1.0. The performance evaluation of our method under facial expression variation is in progress.

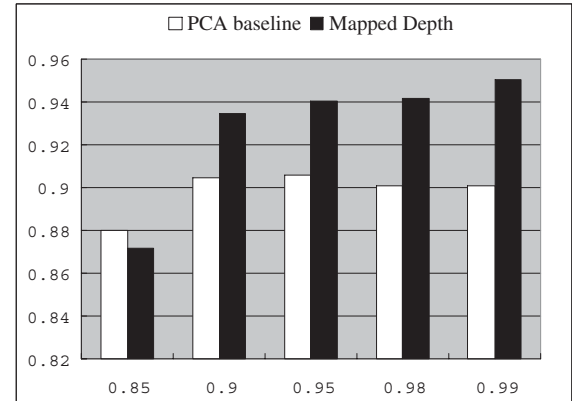


Figure 8: The comparison of rank-1 recognition rate with different rebuilding energy for the proposed method and the PCA baseline. The x-axis is the rebuilding energy, and the y-axis represents the rank-1 recognition rate.

Step	min. of pts 20692	max. of pts 126820
Triangulation	1.875s	14.641s
Finding symmetry plane in Fig.1	1.000s	1.922s
Flattening surface from Fig.4(c) to (f)	1.485s	1.594s
Reference plane detection from Fig.4(c) to (d)	0.000s	0.000s
Regularly resampling in 2D from Fig.4(f) to (g)	0.031s	0.031s

Table 1: Time cost for main steps in our approach. All are carried out by PC with CPU P4 2.4GHz and RAM 512MB.

6 Acknowledgments

The authors are grateful for the grants from the National Science Foundation of China (60273059) and Program for New Century Excellent Talents in University (NCET-04-0545). They would like to thank Dr. Flynn and Dr. Phillips for providing FRGC ver1.0 data set.

References

- [1] R. Chellappa, C. L. Wilson, and S. Sirohey, "Human and machine recognition of faces: A survey," *Proceedings of IEEE*, 83(5):705-740, 1995.
- [2] W. Zhao and R. Chellappa, "Face recognition: A literature survey," *Tech. Rep. CS-TR4167*, University of Maryland, 2000.
- [3] Face Recognition Vendor Test. <http://www.frvt.org/>.
- [4] W. W. Bledsoe, "The Model Method in Facial Recognition," Technical report PRI15. Panoramic Research Inc. Palo Alto, 1966.
- [5] Emanuele Trucco, Alessandro Verri, *Introductory Techniques for 3-D Computer Vision*. Prentice Hall Inc., 1998.
- [6] P. Belhumeur, J. Hespanha, and D. Kriegman, "Eigenfaces vs. fisherfaces: Recognition using class specific linear projection," *IEEE Trans. Pattern Analysis and Machine Intelligence*, 19(7):711-720, 1997.
- [7] John Chun Lee, E. Milius, "Matching Range Images of Human Faces," *Proceedings of IEEE ICCV*, pp.722-726, 1990.
- [8] Gaile.G. Gordon, "Face Recognition based on Depth Maps and Surface Curvature," *Geometric Methods in Computer Vision*, SPIE Proceedings, vol.1570, pp.234-247, 1991.
- [9] Gaile.G. Gordon, "Face Recognition from Depth and Curvature," PhD thesis, Harvard University, Division of Applied Sciences, 1991.
- [10] Y. Yacoob, L.S. Davis, "Labeling of Human Face Components from Range Data," *CVGIP:Image Understanding*, 60(2):168-178, 1994.
- [11] Volker. Blanz, Sami. Romdhani, Thomas. Vetter, "Face Identification across Different Poses and Illumination with a 3D Morphable Model," *Proc. IEEE FGR'02*, pp.202-207, 2002.
- [12] Wenyi Zhao, "Robust Image-based 3D Face Recognition," Ph.D. Thesis, Department of Electrical and Computer Engineering, University of Maryland. College Park, 1999.
- [13] Chin-Seng. Chua, F. Han, Y.K. Ho, "3D human face recognition using point signature," *Proc. IEEE FRG'00*, pp.233-238, 2000.
- [14] C. Beumier, M. Acheroy, "Automatic 3D Face Authentication," *Image and Vision Computing*, 18:315-321, 2000.
- [15] Saad, Youcef, Martin.H. Schultz, "GMRES: A Generalized Minimal Residual Algorithm for Solving Nonsymmetric Linear Systems," *SIAM J. Sci. Stat. Compute.* 7(3):856-869, 1986.
- [16] M.W.Lee, S.Ranganath, "Pose-invariant face recognition using a 3D deformable model," *Pattern Recognition*, 36(8):1835-1846, 2003.
- [17] M. Desbrun, M. Meyer, P. Alliez, "Intrinsic Parametrizations of Surface Meshes," *Proceedings of Eurographics*, 2002.
- [18] A. Gray, *Modern Differential Geometry of Curves and Surfaces*, 2nd edition, CRC Press, 1998.
- [19] M. Meyer, M. Desbrun, P. Schroder, A.H. Barr, *Discrete Differential-Geometry Operators for Triangulated 2-Manifolds*, 2002.
- [20] M.A. Turk, A.P. Pentland, "Face Recognition using Eigenface," *Proc. of Computer Vision and Pattern Recognition*, pp.586-591, 1991.
- [21] R. Barrett, M. Berry, T.F. Chan, etc. "Templates for the Solution of Linear Systems: Building Blocks for Iterative Methods," 2nd Edition, SIAM, Philadelphia, PA, 1994.
- [22] Gang Pan, Zhaohui Wu, Yunhe Pan, "Automatic 3D Face Verification from Range Data," *IEEE ICASSP'03*, vol.3, pp.193-196, 2003.
- [23] Yijun Wu, Gang Pan, Zhaohui Wu, "Face Authentication based on Multiple Profiles Extracted from Range Data," *AVBPA'03, LNCS*, vol.2688, pp.515-522, 2003.
- [24] Gang Pan, Zhaohui Wu, "3D Face Recognition from Range Data," *Int'l Journal of Image and Graphics*, 5(3):573-593, 2005.
- [25] Y. Wang, Gang Pan, Zhaohui Wu, "3D Face Recognition using Local Shape Map," *IEEE ICIP'04*, 2004.
- [26] Xiaoguang Lu, Dirk Colbry, Anil K. Jain, "Three-Dimensional Model Based Face Recognition," *Proc. of ICPR'04*, pp.362-366, 2004.
- [27] A.M. Bronstein, M. M. Bronstein, R. Kimmel, "Expression-invariant 3D face recognition," *AVBPA'03, LNCS*, vol.2688, pp.62-70, 2003.
- [28] Yuxiao Hu, Dalong Jiang, Shuicheng Yan, Lei Zhang, Hongjiang Zhang, "Automatic 3D Reconstruction for Face Recognition," *Proc. IEEE FGR'04*, pp.17-19, Seoul, Korea, 2004.
- [29] P. J. Phillips, P. J. Flynn, T. Scruggs, K. W. Bowyer, J. Chang, K. Hoffman, J. Marques, J. Min, and W. Worek, "Overview of the Face Recognition Grand Challenge," *IEEE Conference on Computer Vision and Pattern Recognition*, 2005.
- [30] H. Hoppe, T. DeRose, T. Duchamp, J. McDonald and W. Stuetzle, "Mesh optimization," *SIGGRAPH'93 Proceedings*, pp.19-26, 1993.